ELSEVIER

Journal of Alloys and Compounds 444–445 (2007) 584–589

Journal of ALLOYS AND COMPOUNDS

www.elsevier.com/locate/jallcom

Alteration of UO_{2+x} under oxidizing conditions, Marshall Pass, Colorado, USA

A.P. Deditius *, S. Utsunomiya, R.C. Ewing

Department of Geological Sciences, University of Michigan, 1100 N. University Avenue, Ann Arbor, MI 48109-1005, United States

Received 20 September 2006; received in revised form 11 January 2007; accepted 3 February 2007
Available online 23 February 2007

Abstract

As a natural analogue of the processes and products of spent nuclear fuel (SNF) alteration, we have examined the sequence of phases that form during the alteration of natural UO_{2+x} in a U-deposit at Marshall Pass, Colorado. We have determined the paragenesis of U(VI)-phases including the fate of trace elements: W, Mo, As, Sb, Cu, Ba, Ce, Y, Pb and Th. Enrichment of trace elements, especially W and Mo, in this system resulted in a unique alteration sequence: uraninite → amorphous U-oxyhydrate gel → schoepite(I)/vandendriesscheite/compreignacite → uranophane → schoepite(II)/"dehydrated" schoepite(I) → Ba–Mo–W–U phase/U-arsenates/U–Sb phase → "dehydrated schoepite" (II) → soddyite/swamboite. In this sequence, the Ba–Mo–W uranyl phase and U–Sb phase are newly characterized phases. These results suggest that the UO_{2+x} alteration, involving higher concentrations of certain radionuclides and metallic compounds, may lead to a different paragenesis of U(VI)-phases, as compared with the expected alteration sequence of UO_2 interacting with a typical groundwaters. This was also noted in a previous study of the alteration of Pb-rich uraninite [R.J. Finch, R.C. Ewing, J. Nucl. Mater. 190 (1992) 133–156]. Some trace elements, such as CaO 2.08 wt.%, PbO 1.69 wt.%, WO_3 1.39 wt.%, As_2O_3 0.50 wt.% and MoO_3 0.41 wt.%, can locally concentrate, but still form uranyl phases. As a consequence, the mobility of U and radionuclides is governed by the stability of these metal-uranyl phases, such as Pb-oxide hydrates, Ba-uranyl molybdates/ tungstates and U-antimonate.

Keywords: Actinide alloys and compounds; Crystal structure; Corrosion; Oxidation

1. Introduction

Under oxidizing conditions, the alteration and corrosion of spent nuclear fuel (SNF) leads to the release of actinides and the fission products such as: U, Np and Mo, Tc, Ru, Rh, Pd, Rb, Cs, Ba, Zr, Sr, and Nb. The released elements may be mobile if they remain in solution, or they may be incorporated into the alteration phases by co-precipitation or sorbed onto the surfaces of corrosion products and minerals [2–4]. Thus, it is important to evaluate the fate of these radionuclides under repository conditions. The structure and composition of the SNF is similar to young low-Pb uraninites (UO_{2+x}) [5], and there are many similarities in the sequence of U(VI)-phases that form during alteration [6–9]. Thus, studies of natural systems in which uraninite has been altered provide information about the long-term alteration of UO_2.

The uranium deposit at Marshall Pass, Colorado, formed along a pre-Tertiary fault system as a result of the interactions between migrating hydrothermal fluids and host rocks. Complex tectonic deformation caused thrusting of the Proterozoic crystalline rocks (gneisses, granites) over the Paleozoic sedimentary sequence (quartzite, dolomite). This assemblage is uncomformably covered by Tertiary tuffs and andesite, which are suggested to be the main source of uranium [10]. Primary uraninite was formed under reducing conditions in veins controlled by the pattern of faults. The UO_{2+x} formed with Cu, Zn, Pb, Sb, Ag and As sulfides and sulfosalts, such as tetrahedrite [$(Cu,Fe,Ag,Zn)_{12}Sb_4S_{13}$], covellite [CuS], chalcocite [Cu_2S], chalcopyrite [$CuFeS_2$], galena [PbS], and sphalerite [ZnS] [11]. The hydrothermal U-ore deposit is located close to the surface and has reacted with subsurface ground water, mixed with oxidizing meteoric waters. As with the Nopal I deposit [8] and

* Corresponding author. Tel.: +1 734 763 5344; fax: +1 734 647 5704.
E-mail address: deditius@umich.edu (A.P. Deditius).

0925-8388/$ – see front matter © 2007 Elsevier B.V. All rights reserved.
doi:10.1016/j.jallcom.2007.02.095

laboratory experiments of SNF corrosion [6,7], the Marshall Pass deposit is in the unsaturated zone under oxidizing conditions.

The U(VI)-minerals typically consist of sheet-like structures of edge-sharing UO_2^{2+} polyhedra. The complexity of the U(VI)-mineral structures provides many possibilities for coupled-substitutions of trace metals and radionuclides [2,12,13]. Recently, substantial attention has been focused on U(VI)-phases and their capacity for the incorporation of trace elements as a mechanism that may reduce the mobility of certain radionuclides once released from SNF [3,4,14]. In this study, we examined the alteration of natural UO_{2+x} in order to understand the sequence of U(VI)-phases that form under oxidizing conditions in a rather unique chemical system, which includes: W, Mo, As, Sb, Cu, Ba, Ce, Y, Pb and Th.

2. Analytical methods

Five samples, with different degrees of alteration, were analysed using scanning electron microscopy/energy dispersive X-ray spectrometry (SEM/EDS, Hitachi S3200N) and electron microprobe analysis (EMPA, a Cameca SX100). EMPA point analyses were completed using an accelerating voltage of 20 kV and beam current of 40 nA. A counting time of 120 s was used to improve the statistics of the count rates. The standards used for the calibration were: zircon ($ZrSiO_4$) for Zr (L_α), scheelite ($CaWO_4$) for W (M_β), andradite ($Ca_3Fe_2Si_3O_{12}$) for Si (K_α), Ca (K_α) and Fe (K_α), albite ($NaAlSi_3O_8$) for Al (K_α and K_β), benitoite ($BaTiSi_3O_9$) for Ba (L_α), synthetic UO_2 for U (M_β), synthetic $KTaO_3$ for K (K_α), synthetic YPO_4 for Y (L_α), synthetic $KTiO_3$ for Ti (K_α), thorite ($ThSiO_4$) for Th (M_α), cerussite ($PbCO_3$) for Pb (M_α), synthetic $CaMoO_4$ for Mo (L_α), synthetic YPO_4, $LaPO_4$ or $CePO_4$ for P (K_α), synthetic covellite CuS for Cu (K_α).

High-resolution transmission electron microscopy (HRT-EM), analytical electron microscopy (AEM), and high-angle annular dark-field scanning transmission electron microscopy (HAADF-STEM) were conducted using a JEOL JEM2010F. The spherical coefficient C_s is 1.0 mm. In STEM mode, the probe size was 1.0 nm, and the collection angle of the HAADF detector was 50–110 mrad. The size of condenser aperture was 20 μm.

3. Results and discussion

3.1. Sequence of uranyl alteration phases in Marshall Pass

The chemical composition of primary colloform uraninite, determined by EMPA, is 85.2–89.0 wt.% UO_2, 0.82–2.84 wt.% CaO, 0.97–2.51 wt.% PbO, 1.04–2.15 wt.% WO_3, 0.32–1.30 ZrO_2 and 0.15–1.7 wt.% As_2O_3, with minor amounts (<1 wt.%) of Ti, REE, Mo, Si, P and Fe (Table 1). These primary uraninites formed in fluids with a relatively high concentration of W, which is incorporated into the interstitial sites of uraninite structure.

The first stage of alteration was caused by penetration of oxidizing fluids containing Pb and Mo. The oxidation of U may have caused shrinkage of the uraninite unit cell, which, in turn, created microfractures. Uraninite grains are brecciated (Fig. 1a).

Table 1
Electron microprobe analyses of uranium minerals from Marshall Pass, Colorado, USA

Mineral	uraninite	uranyl oxide-hydrates				uranophane	soddyite	swamboite	U-arsenates	U-amorph	Ba–Mo–W–U phase	U–Sb phase
		vandendriescheite	schoepite	dehydr. schoepite	compreignacite							
Anal #	#58	#3	#33	#22	#11	#12	#13	#24	#17	#16	#29	#8
Al_2O_3	0.155	n.d.	n.d.	n.d.	0.023	n.d.	n.d.	n.d.	n.d.	0.319	0.046	n.d.
SiO_2	0.484	0.241	0.494	0.274	0.384	13.921	8.760	13.994	0.571	1.251	0.228	0.275
P_2O_5	0.097	n.a.	0.106	n.d.	0.041	0.017	0.022	0.169	0.972	0.228	0.085	n.d.
K_2O	0.390	1.030	0.432	2.128	2.532	1.232	0.882	1.444	0.617	0.925	0.997	1.468
CaO	2.081	0.804	1.489	0.023	0.276	5.991	n.d	0.188	0.181	1.542	0.670	0.873
TiO_2	0.262	0.102	0.290	0.018	0.078	n.d.	0.016	0.015	0.014	0.772	2.411	n.d.
Fe_2O_3	0.300	0.073	0.190	n.d	0.066	n.d.	n.d.	n.d.	n.d.	0.508	1.307	1.199
As_2O_3	0.504	1.657	0.985	0.035	1.096	1.307	0.096	0.484	16.650	1.001	0.639	2.062
Y_2O_3	0.136	n.d.	0.099	n.d.	n.d.	n.d	n.d.	n.d.	n.d.	0.034	n.d.	0.328
ZrO_2	0.566	0.025	1.144	n.d.	n.d.	n.d	n.d.	n.d.	n.d.	1.485	0.237	n.d.
MoO_3	0.410	1.153	0.646	0.059	0.182	0.123	n.d.	0.041	0.298	1.118	11.285	0.050
Ce_2O_3	0.088	0.031	0.104	n.d.	n.d.	n.d.	n.d.	n.d.	n.d.	0.079	0.488	0.495
WO_3	1.394	0.815	1.488	0.054	0.379	1.167	0.698	1.147	0.057	3.226	12.578	n.d.
Sb_2O_3	n.a.	n.a.	n.a.	n.a.	n.a.	n.a.	n.a.	n.a.	n.a.	n.a.	n.a.	28.493
BaO	n.d.	n.d.	n.a.	n.a.	n.a.	n.a.	n.a.	n.a.	n.a.	n.a.	4.481	n.d.
CuO	n.a.	n.a.	n.a.	n.a.	n.a.	n.a.	n.a.	n.a.	1.818	n.a.	n.a.	3.349
PbO	1.685	7.647	2.306	0.255	2.043	n.d.	0.063	0.480	0.110	0.396	0.291	3.512
ThO_2	n.d.	n.d.	n.d	n.d.	n.d.	n.d.	0.004	0.019	n.d.	0.032	0.052	n.d.
UO_2	86.984	80.951	83.868	91.737	86.472	71.466	82.271	75.496	69.798	71.508	56.851	53.865
Total	95.371	94.534	93.651	94.612	93.591	95.251	92.844	93.502	90.875	85.556	93.457	96.582

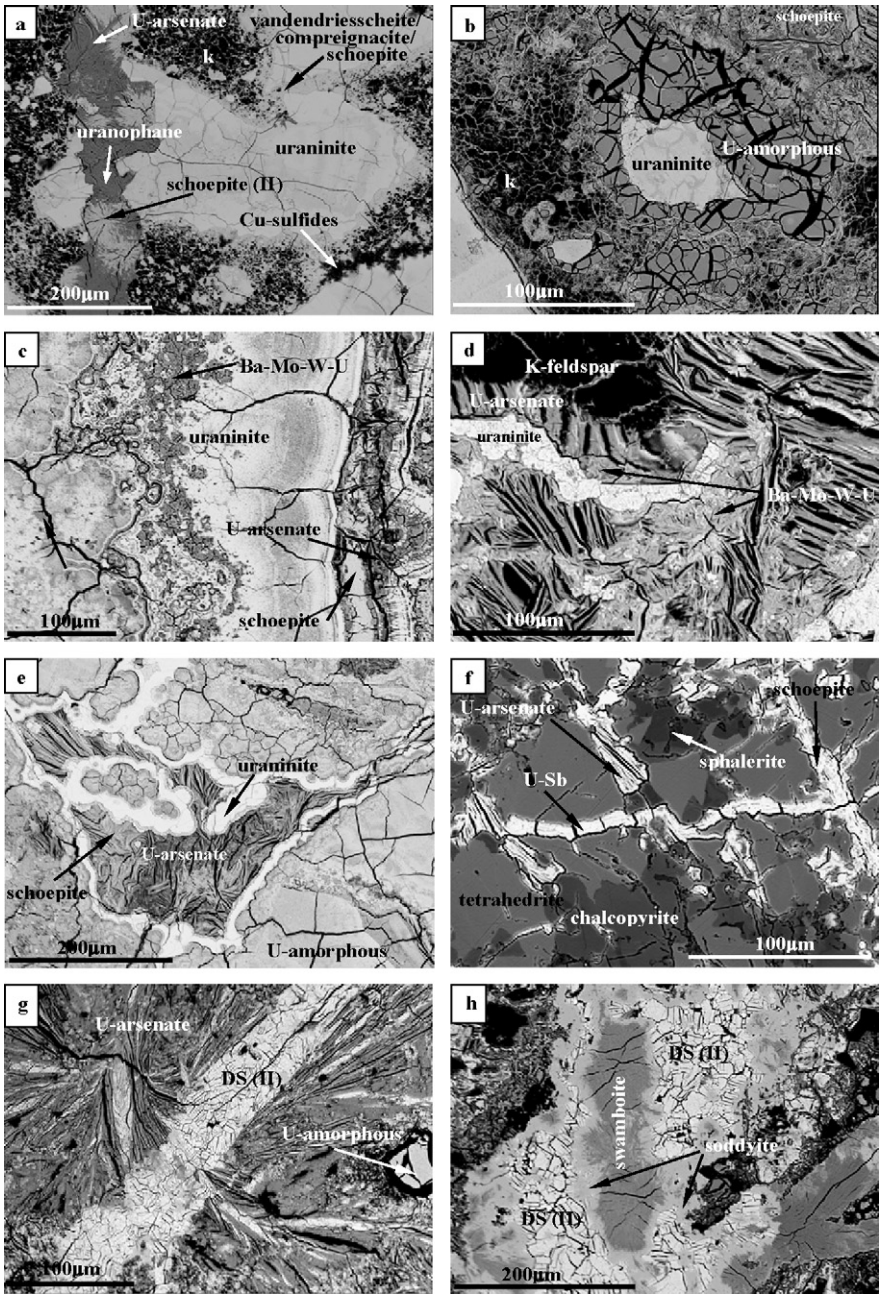

Fig. 1. BSE images of colloform uraninite and paragenesis of U(VI)-phases. (a) Fragment of the colloform uraninite within kaolinite (*k*) with rim consisting of a mixture of schoepite, vandendriescheite and compreignacite; uraninite grain is cut by vein with uranophane which was subsequently replaced by schoepite (II) and U-arsenates; (b) uraninite replaced by amorphous U-oxide hydrate gel phase associated with fractures filled with silica; (c) Ba–Mo–W uranyl phase within the colloform uraninite; (d) coexistence of U-arsenates and Ba–Mo–W uranyl phase replacing a primary K-feldspar; (e) U-arsenate replacing schoepite in the void of colloform uraninite growing on the U-amorphous phase; (f) tetrahedrite cut by vein filled with U–Sb phase; (g) secondary "dehydrated schoepite" (DS II) replacing U-arsenates; (h) swamboite precipitated at the expense of DS (II). Note the precipitation of soddyite between DS(II) and swamboite.

Sulfides and sulfosalts are unstable under oxidizing conditions, and the dissolution of the sulfides released Pb, As, Cu, Zn, Sb, Ag and S, acidifying the fluids. The presence of Mo in the fluids with released Pb resulted in precipitation of wulfenite [$PbMoO_4$].

The sequence of U(VI) phases that formed during alteration began with yellowish U-oxide hydrous gel (identified by HRTEM) and then a dark yellow to brownish rim of schoepite [$(UO_2)_8O_2(OH)_{12}\cdot 12(H_2O)$] surrounding the uraninite + U-oxide gel, followed by "dehydrated" schoepite (I), which is intergrown with rare Pb-uranyl oxide hydrates, most likely vandendriesscheite [$Pb_{1.57}(UO_2)_{10}O_6(OH)_{11}(H_2O)_{11}$] and compreignacite [$K_2(UO_2)_6O_4(OH)_6(H_2O)_7$] (Fig. 1a, Table 1). However, the EMPA does not allow for the definite identification of these intergrown phases. Subsequently, mats of fine-grained platy crystals of a Ba–Mo–W–U phase formed with chemical composition varying in the range: 54.7–62.6 wt.% of UO_2, 8.04–19.03 wt.% of WO_3, 8.61–16.4 wt.% of MoO_3, 4.06–5.07 wt.% of BaO,

2.02–2.75 wt.% of TiO_2, 0.87–1.89 wt.% of Fe_2O_3, 0.34–0.96 wt.% of CaO, and 0.31–0.71 wt.% of Ce_2O_3, (Table 1; Fig. 1c).

At the next stage of alteration, fluids containing Si and Ca caused the precipitation of uranophane [$Ca(UO_2)_2(SiO_3OH)_2(H_2O)_5$], followed by precipitation of uranyl arsenates, mainly trogerite [$(UO_2)_3(AsO_4)_2(H_2O)_{12}$], as well as a lesser amount of (meta)zeunerite, [$Cu[(UO_2)(AsO_4)]_2(H_2O)_8$] (Fig. 1a, d and e). A different paragenesis was observed in the areas where sulfides and sulfosalts are adjacent to uraninite. The Cu-bearing minerals, which are unstable under oxidizing conditions (tetrahedrite, covellite, chalcocite, chalcopyrite), dissolved, as evidenced by corrosion rinds, and this provided various trace metals such as Cu, As and Sb for the subsequent precipitation of uranyl minerals (Fig. 1f). As a result (meta)zeunerite precipitated replacing uraninite and the Cu-minerals. A thin layer (2–5 μm) of a fine-grained unknown phase was found between uraninite, U-arsenate and tetrahedrite. The unknown phase is optically transparent and enriched in UO_2 (50.6–55.8 wt.%) and Sb_2O_3 (26.9–31.3 wt.%).

The last stage of alteration was caused by reaction with meteoric water. U-arsenates and silicates were replaced by "dehydrated schoepite" (II) (Fig. 1g). Finally, the "dehydrated schoepite" was altered to swamboite [$U^{6+}(UO_2)_6(SiO_3OH)_6(H_2O)_{30}$] via soddyite [$(UO_2)_2(SiO_4)(H_2O)_2$] (Fig. 1h, Table 1). This sequence is in good agreement with thermodynamic estimates for the SiO_2–UO_3–CaO–H_2O system by Ref. [15], which illustrated that swamboite and dehydrated schoepite are separated by the stability field of soddyite [$(UO_2)_2(SiO_4)(H_2O)_2$].

3.2. Comparisons with occurrence at Nopal I, Peña Blanca, Mexico and laboratory results

A chart of the paragenesis of U(VI) phases characterized in this study is summarized in Fig. 2 and compared with previous studies [12,13,16]. In general, the first stages of the U(VI)-phase paragenesis in the Marshall Pass deposit are comparable to that observed in the Nopal I deposit (Mexico) and laboratory corrosion experiments: uraninite → uranyl oxide hydrates → uranyl silicates → alkali + alkali earth uranyl silicates [7,8]. The differences in paragenesis are mainly caused by chemical composition of the primary uraninite and the chemistry of oxidizing fluids. There are trace amounts of Si, Ca, K, S and Na in the hydrothermal uraninites at the Nopal I deposit [8], but no Mo and REEs, which are typical fission product elements found in SNF. The groundwater in Nopal I is reported to be enriched in SO_4^{2-}, Ca^{2+}, Na^+ and Si^{4+} [8]. The starting material in the corrosion experiments [7] was synthetic UO_2, which was reacted with the simulated Yucca Mountain groundwater, EJ-13 enriched in, Na, Si, Ca and K [7]. On the contrary, the primary UO_{2+x} in Marshall Pass is enriched with W, Mo, Zr and As and also contains relatively small amounts of Ce and Y (Table 1).

The first difference between the Marshall Pass deposit, Nopal I deposit, and laboratory results is the formation of the amorhous U-oxide gel, which can be considered to be part of the initial "uranyl oxide hydrate stage" [7–9]. The K^+ in the system resulted in local precipitation of compreignacite, similar to the observed conversion of schoepite to compreignacite in the UO_2 drip tests [7]. Radiogenic Pb^{2+} from the uraninite and sulfides precipitated vandendriesscheite [$Pb_{1.57}(UO_2)_{10}O_6(OH)_{11}(H_2O)_{11}$], which is consistent with [1,17]. Predominance of uranophane, sklodowskite [$Mg(UO_2)_2(SiO_3OH)(H_2O)_6$], Na-boltwoodite [$K(UO_2)_2(SiO_3OH)(H_2O)_{1.5}$], and weeksite [$K_{1-x}Na_x(UO_2)_2(Si_5O_{13})(H_2O)_4$] observed in previous studies [7,8] was not observed in Marshall Pass deposit. The absence of the aforementioned phases is attributed to the relatively low Ca, Na and Si activities in the fluids during the early stage of alteration. This is consistent with the very rare occurrence of uranophane, and its replacement by secondary schoepite (Fig. 1a).

The main stage of alteration in the present samples was the precipitation of the uranyl arsenates and a Ba–Mo–W–U phase, which replaced the pre-existing phases. The only corresponding

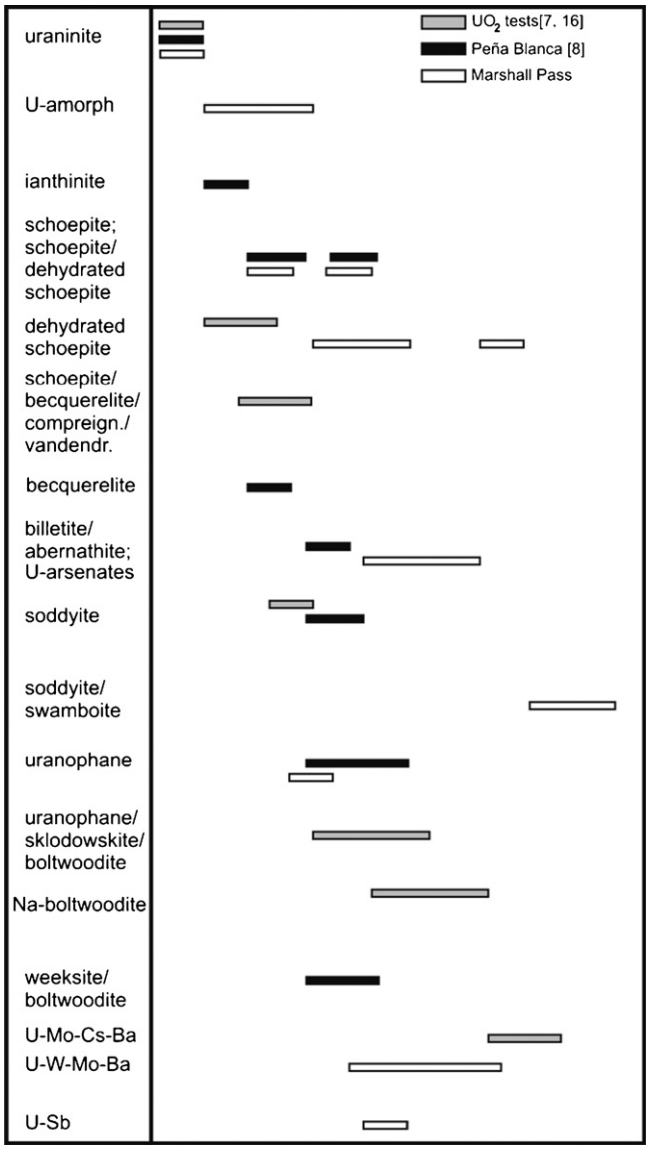

Fig. 2. Comparison of the alteration sequence observed at Marshall Pass, Colorado, with the Nopal I, Peña Blanca, and laboratory corrosion experiments [7,8,16].

phases in the Nopal I deposit are abernathite $[K_2[(UO_2)_2(AsO_4)]_2(H_2O)_8]$ and billetite $[Ba(UO_2)_6O_4(OH)_6(H_2O)_8]$, respectively, which are present as minor phases in the alteration sequence [6]. In the oxidative corrosion experiments of SNF, Cs–Ba uranyl molybdate $[(Cs_{0.8}Ba_{0.6})(UO_2)_5(MoO_2)O_4(OH)_6(H_2O)_n]$ was identified [6,16]. This Cs–Ba uranyl molybdate phase may closely correspond to the Ba–Mo–W–U phase in the present study. We have also characterized a U–Sb phase that precipitated in the vicinity of tetrahedrite, which is a newly reported phase in the UO_2 alteration sequence. This occurrence confirms the importance of WO_2^{2+} and MoO_2^{2+} complexes in the retardation of uranium at the Marshall Pass deposit.

The final stages of alteration, which include the formation of dehydrated schoepite and the sequence from dehydrated schoepite through soddyite to swamboite, have not been previously reported. The later sequence from dehydrated schoepite to swamboite via soddyite is similar to the first stages of UO_2 alteration in the previous studies [6–8], where schoepite and dehydrated schoepite are altered to soddyite followed by uranyl alkaline silica hydrates.

3.3. New uranyl phases

The chemical formula of the Ba–Mo–W–U phase, normalized to eight oxygen atoms is: $(Ba^{2+}_{0.23}K^{+}_{0.17}Fe^{3+}_{0.13}Ca^{2+}_{0.10}Cu^{2+}_{0.08}Ce^{3+}_{0.02}Pb^{2+}_{0.01})_{0.74}Ti^{4+}_{0.24}(Mo^{6+}_{0.63}W^{6+}_{0.43}O_{4.00})_{1.06}(UO_2)_{1.68}(OH)_{11.64}(H_2O)_n$. The simplified formula is: $Ba_2(UO_2)_5Ti[(Mo,W)O_4]_3(OH)_{12}(H_2O)_n$.The Ba^{2+} is the major interlayer cation, while K, Rb and Ti provide links between sheets of the Ba–Mo–W–U phase. The only known Ba–W-rich uranyl mineral is orthorhombic uranotungstite [18] $[(Ba,Pb,Fe^{2+})(UO_2)_2(WO_4)(OH)_4(H_2O)_{12}]$. However, neither Mo^{6+} nor Ti^{4+} was reported in this mineral, and its structure has not yet been fully determined [18]. The cleavage structure of the Ba–Mo–W–U phase (Fig. 1c) indicates that this phase is a sheet-type uranyl phase. The position of Ti^{4+} is problematic in this Ba–Mo–W–U phase. The relatively high valence state of $Ti^{(4+)}$ requires the Ti atoms to occupy the octahedral sites of the structure, which occur in the uranyl compound $[(UO_2)TiNb_2O_8]$ [2,19].

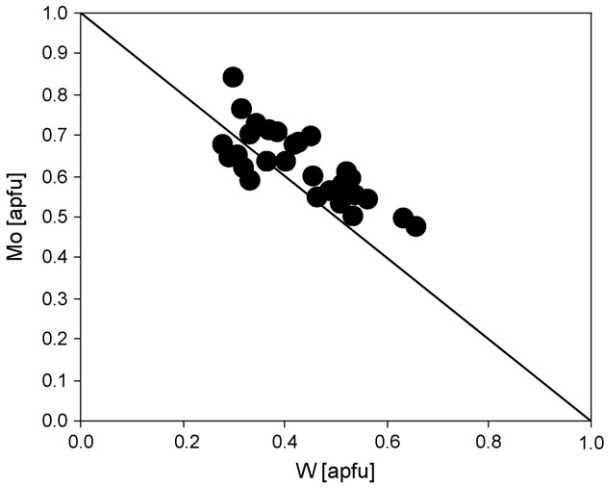

Fig. 3. Negative linear correlation between Mo [apfu] plotted against W [apfu] in the Ba–Mo–W uranyl phase.

A negative correlation between Mo and W in Ba–Mo–W–U phase suggests a possible substitution, according to Mo_xW_{1-x}, in the structure of this phase (Fig. 3). The ratio of U:Mo(+W) is a useful parameter for determining the Ba–Mo–W–U phase stoichiometry. The ratio is approximately 5:3 for the present phase, while most uranyl molybdates have a U:Mo ratio of $\geq$1:1. The structure of tungstates and molybdates are constrained to the anion topology of sheet structures that consist of triangles, squares and pentagons; thus, this ratio becomes $\geq$2:1 [2]. The Mo $\leftrightarrow$ W substitution in this phase is supported by the closely related structures of two uranyl compounds, $[Tl_2[(UO_2)_2O(MoO_5)]$ and $[(K,Rb)_2[(UO_2)_2O(WO_5)]$ [2,20,21]. Both structures are based on $[(UO_2)_2O(WO_5)]$ sheets with the same topology. MoO_5 polyhedra have tetragonal pyramidal and trigonal bipiramidal geometry [20], while WO_5 polyhedra occur only as distorted square pyramids [21]. Alekseev et al. [22] also reported the same WO_5 polyhedra and proposed that the replacement of Mo^{6+} by W^{6+} can cause some distortion of coordination polyhedra. The present Ba–Mo–W–U phase is also comparable to the synthetic compound $[(Ag,Na)_{10}[(UO_2)_8O_8(Mo_5O_{20})]$, which belongs to the wölsendorfite anion-topology [12]. Mo and W are located in the MoO_6 and WO_6 octahedra in the structure of the synthetic compounds, forming Mo_5O_{20} or W_5O_{20} clusters [2,21,23].

Consideration of the chemical composition and possible crystal-chemistry of Ba–Mo–W–U phase reveals two interesting aspects of the SNF alteration process. First, the Ba–Mo–W–U phase may retard migration of U and fission products, such as ^{137}Ba, ^{93}Mo and minor amounts of REE^{3+}. Second, the U:(Mo + W) ratio of 5:3 in the present phase is comparable to the U:Mo ratio of 2:1 in $(Cs_{0.8}Ba_{0.6})(UO_2)_5(MoO_2)O_4(OH)_6(H_2O)_n$, which is the phase previously observed during SNF corrosion tests [16]. The structure of the Cs–Ba–Mo uranyl oxide hydrate characterized in the SNF corrosion experiments has two unique uranyl oxide sheets: (i) one sheet with edge sharing $Ur\varphi_5$ polyhedra with the composition of $(UO_2)_6O_4(OH)_6$ and another sheet, $(UO_2)_4(MoO_2)_2O_4(OH)_6$, possessing $Ur\varphi_5$ and $Ur\varphi_4$ pentagonal bipiramids and octahedra [16]. The large Cs^+ and Ba^{2+} ions occupy interlayer positions and are coordinated by at least seven ligands that contain H_2O and O_{Ur} (apical oxygen of uranyl ion) [12].

The second new uranium phase found in this study is a U-antimonate phase. The U:Sb atomic ratio in the U–Sb phase is about 1:1. Some uncertainties are introduced by the relatively high concentrations of CuO (3.35 wt.%), PbO (3.51 wt.%), As (2.06 wt.%), and Fe_2O_3 (1.20 wt.%). $USbO_5$ was previously synthesized [24,25], and the oxidation state of U was determined to be 5+, which suggests that U is coordinated by seven O into pentagonal bipiramids, and Sb^{5+} is located in the center of SbO_6 octahedra. Thus, Sb can play a key role in stabilizing UO_2^+ ion in anoxic, U-rich waters.

4. Conclusions

Oxidizing fluids of different compositions caused a complex sequence of alteration phases in Marshall Pass, Colorado, resulting in significant differences in the paragenesis of secondary uranyl mineral as compared with previous results of the laboratory corrosion tests of SNF and in the Nopal I deposit, Mexico. The differences are as follows: (i) Amorphous U-oxide gel formed during the initial "uranyl oxide hydrate stage"; (ii) Formation of Ba–Mo–W uranyl phase after the hydrous uranyl-oxides stage. This phase may incorporate fission products such as ^{137}Ba, ^{137}Cs, ^{93}Mo, ^{90}Sr and REE^{3+} [2,22]; (iii) Locally high concentrations of Sb resulted in precipitation of a new U–Sb phase, which suggest that Sb can also stabilize the UO_2^+ ion; (iv) Uranyl arsenates are major phases in this system, having been replaced by meta-stable U-oxide hydrates, and subsequently, by soddyite and swamboite.

Acknowledgements

The authors are grateful to the L. Shuller for her careful review of this manuscript. This work was supported by the Office of Science and Technology and International (OST&I) of the Office of Civilian Radioactive Waste Management (DE FC28 04RW12254). The views, opinions, findings and conclusions or recommendations of the authors expressed herein do not necessarily state or reflect those of DOE/OCRWM/OSTI.

References

[1] R.J. Finch, R.C. Ewing, J. Nucl. Mater. 190 (1992) 133–156.
[2] P.C. Burns, Can. Miner. 43 (2005) 1839–1894.
[3] P.C. Burns, R.J. Finch, F.C. Hawthorne, M.L. Miller, R.C. Ewing, J. Nucl. Mater. (1997) 199–206.
[4] P.C. Burns, K.M. Deely, S. Skantharkumar, Radiochim. Acta 92 (2004) 151–159.
[5] J. Janeczek, R.C. Ewing, V.M. Oversby, L.O. Werme, J. Nucl. Mater. 238 (1996) 121–130.
[6] R.J. Finch, E.C. Buck, P.A. Finn, J.K. Bates, Mater. Res. Soc. Symp. Proc. 556 (1999) 431–437.
[7] D.J. Wronkiewicz, J.K. Bates, S.F. Wolf, E.C. Buck, J. Nucl. Mater. 238 (1996) 78–95.
[8] E.C. Pearcy, J.D. Prikryl, W.M. Murphy, B.W. Leslie, Appl. Geochem. 9 (1994) 713–732.
[9] D.J. Wronkiewicz, J.K. Bates, T.J. Gerding, E. Veleckis, J. Nucl. Mater. 190 (1992) 107–127.
[10] J.C. Olson, U.S. Geological Surv. Prof. Pap. 1457 (1988) 1–44.
[11] D. Zhao, R.C. Ewing, Radiochim. Acta 88 (2000) 739–749.
[12] P.C. Burns, in: P.C. Burns, R. Finch (Eds.) Rev. Miner. Geochem. (1999) 23–90.
[13] R. Finch, T. Murakami, in: P.C. Burns, R. Finch (Eds.) Rev. Miner. Geochem. (1999) 91–180.
[14] P.C. Burns, R.C. Ewing, M.L. Miller, J. Nucl. Mater. 245 (1997) 1–9.
[15] R.J. Finch, Mater. Res. Soc. Symp. Proc. 465 (1997) 1185–1192.
[16] E.C. Buck, D.J. Wronkiewicz, P.A. Finn, J.K. Bates, J. Nucl. Mater. 249 (1997) 70–76.
[17] R.J. Finch, R.C. Ewing, Mater. Res. Soc. Symp. Proc. 257 (1992) 465–472.
[18] K. Walenta, Tschermaks Miner. Petrol. Mitt. 34 (1985) 25–34.
[19] R. Chevalier, M. Gasperin, C.R. Acad. Sci. C267 (1969) 1426–1428.
[20] S. Krivovichev, P.C. Burns, Can. Miner. 41 (2003) 1225–1231.
[21] S. Obbade, C. Dion, E. Bekaert, S. Yagoubi, M. Saadi, F. Abraham, J. Solid State Chem. 172 (2003) 305–318.
[22] E.V. Alekseev, S.V. Krivovichev, W. Dempmeier, T. Armbruster, H. Katzke, E.V. Suleimanov, E.V. Chupronov, J. Solid State Chem. 179 (2006) 2977–2987.
[23] S. Krivovichev, P.C. Burns, Can. Miner. 41 (2003) 1455–1462.
[24] R.K. Graselli, D.D. Surech, K. Knox, J. Catal. 18 (1970) 356–358.
[25] P.G. Dickens, G.P. Stuttard, J. Mater. Chem. 2 (1992) 691–694.